Analysis of Gene Regulatory Network Motifs in Evolutionary Development of Multicellular Organisms

Lisa Schramm[1], Vander Valente Martins[2], Yaochu Jin[3,*] and Bernhard Sendhoff[4]

[1]Technische Universität Darmstadt, Karolinenplatz 5, 64289 Darmstadt, Germany
[2]Escola Politécnica da Universidade de São Paulo, Av. Prof. L. Gualberto, trav. 3, 380, 05508-970 São Paulo, Brazil
[3]University of Surrey, Guildford, Surrey, GU2 7XH, UK
[4]Honda Research Institute Europe, Carl-Legien-Str. 30, 63073 Offenbach, Germany
lschramm@rtr.tu-darmstadt.de

Abstract

Biological development is governed by gene regulatory networks (GRNs), although detailed genetic and cellular mechanisms remain unclear. By means of analyzing biological data, it is believed that some GRN motifs have played an important role in the evolution of biological development. In this work, we investigate in a computational model for development to verify if these motifs can also be evolved as in biology, which can not only help understand biological development and improve simulated evolution as well. The goal of the evolution is to evolve an elongated body plan using a cellular developmental model controlled by a GRN. We count the number of network motifs during the evolution and try to relate the changes of these network motifs to the fitness profile of the evolution. We find for the number of most motifs an increase in the beginning of the evolution and a decrease as the evolution proceeds. We hypothesize that at the beginning a high number different motifs is helpful for the evolution, however, motifs that are not used for the targeted development, i.e., an elongated body morphology in this work, will get lost later on. Finally, we examined two individuals before and after a fitness jump to analyze which genetic changes have contributed to the large fitness improvement.

Introduction

Recent advances in computational systems biology suggest that computational models for development may help us to gain more insights into the genetic and cellular mechanisms underlying biological development. Among other research efforts, analysis of small, frequently occurred network structures, often known as network motifs, have attracted much interest as described by Alon (2007, 2006). Analysis of biological data revealed that such motifs can widely be identified in bacteria and yeast, see e.g., Babu et al. (2004). Most recently, it has been found that some motifs may have played an essential role in evolution. For instance, Kwon and Cho (2008) analyzed the role of feedback loops and found that more positive feedback loops and less negative feedback loops contribute to the robustness of the regulatory system.

However, the analysis of motifs on an evolutionary scale requires the data of many individuals from different evolutionary stages. These data are (currently) not available in biology. Therefore, it seems advisable to support the biological analysis with the results from computational models. Even though these models are usually abstract and the analysis is computationally expensive, it is the target to identify patterns that relate the emergence of motifs to the evolutionary progress in computational models.

Some computational models for artificial development have been proposed (see Harding and Banzhaf (2008)) based on various computational models of GRNs (de Jong, 2002; Geard and Willadsen, 2009). In models of artificial development, one or a few single cells divide and proliferate in a 2D or 3D environment. These cells interact with each other, developing into a pattern, a structure or a shape.

One major concern in cell-based developmental models under the control of GRNs is a self-stabilizing cell growth and the ability to self-heal after a damage. The French flag problem is a popular benchmark used in artificial development, see e.g., Joachimczak and Wròbel (2009); Wolpert (2004). Andersen et al. (2009) managed to evolve a stable development and demonstrate the capacity of self-repair using a GRN based on cellular automata. In their model, cells are fixed on a grid and contact inhibition is adopted, i.e., if a cell is surrounded by other cells, it will not divide any more.

In this work, we have used a cellular growth model described by Steiner et al. (2007), which was inspired by an artificial development model suggested by Eggenberger Hotz et al. (2003). We use a GRN network model that defines the actions of the cells. The cells interact with each other through diffusion of external transcription factors. In contrast to other work, our cells are not fixed on a grid and can move via cell-cell physical interactions. In addition, cells can divide as long as the gene for cell division is active. Therefore, the model has fewer assumptions and the developmental process is less constrained. This model has been employed for simulating neural development in a hydra-like animat (Jin et al., 2008). Stable cell growth has also evolved in a co-evolution of morphology and control of swimming
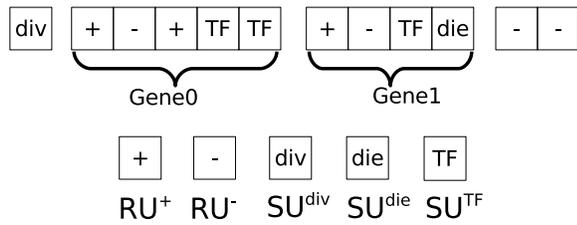
Figure 1: An example chromosome for the development.

animats (Schramm et al., 2009). Additionally, stable and lightweight structures have evolved in (Steiner et al., 2009) using this cellular model.

In (Steiner et al., 2007), the authors showed that the emergence of a negative feedback motif helps to enhance the mutational robustness. In this paper, we analyze the motifs of the GRNs in the best individuals of the whole evolutionary run to see how various network motifs have contributed to the evolution of cellular development. We examine the change in the number of motifs during evolution. Additionally, we analyze the difference in the structure of the GRNs of two related individuals before and after a fitness jump.

We describe our model in the next section followed by an introduction to the widely studied network motifs. Then we present the experimental results of the evolutionary runs together with the number of motifs during the evolution. We conclude the paper with an analysis of two individuals, a summary and an outlook.

The Computational Model for Morphological Development

The morphological development starts with a single cell that can perform a few cellular actions, e.g. cell division or cell death. The cell is placed in the center of a two-dimensional computation area of size 100×80, the cells are not fixed on a grid and can be at all positions inside the computation area. The cells interact physically with each other and can produce transcription factors (TFs) that are used for cell-cell communication. A gene regulatory network (GRN) defines the behavior of the cells.

The genes of the virtual DNA in each cell consist of regulatory units (RUs) and structural units (SUs), see Schramm et al. (2009) for details, as illustrated in Figure 1. The SUs of a gene define the cellular behaviors, in this paper cell division, cell death or the production of TFs. The RUs define whether a gene is activated (expressed). All RUs have an activation level depending on the TF concentrations inside and outside a cell. The activation of a gene is defined by a sum of the activation levels of its RUs, which can be activating (RU^+) or inhibiting (RU^-). If the difference between the affinity values of a TF and a RU is smaller than a predefined threshold ϵ (in this work ϵ is set to 0.2), the TF can bind to the RU to regulate the gene activation. The affinity

similarity $(\gamma_{i,j})$ between the i-th TF and j-th RU is defined by:

$$\gamma_{i,j} = \max\left(\epsilon - \left|\mathrm{aff}_i^{TF} - \mathrm{aff}_j^{RU}\right|, 0\right). \tag{1}$$

If $\gamma_{i,j}$ is greater than zero, then the concentration c_i of the i-th TF is checked whether it is above a threshold ϑ_j defined in the j-th RU:

$$b_{i,j} = \begin{cases} \max(c_i - \vartheta_j, 0) & \text{if } \gamma_{i,j} > 0 \\ 0 & \text{else} \end{cases}. \tag{2}$$

Thus, the activation level contributed by the j-th RU (denoted by $a_j, j = 1, ..., N$) can be calculated as follows:

$$a_j = \sum_{i=1}^{M} b_{i,j}, \tag{3}$$

where M is the number of TFs that bind to the j-th RU. Assume the k-th gene is regulated by N RUs, the expression level of the gene can be defined by a summation of the activations of all RUs

$$\alpha_k = 100 \sum_{j=1}^{N} h_j a_j (2s_j - 1), \ s_j \in (0, 1). \tag{4}$$

$2s_j - 1$ denotes the sign (positive for activating and negative for repressive) of the j-th RU and h_j is a parameter representing the strength of the j-th RU. The k-th gene is activated if $\alpha_k > 0$ and its corresponding behaviors coded in the SUs are performed.

The SU for cell division (SU$^{\mathrm{div}}$) encodes where the new cell is placed in comparison to the mother cell. A cell with an activated SU for cell death dies at the developmental timestep which it is activated. When SUs for both cell death and cell division are simultaneously active, the cell dies without division. Two additional SUs are reserved for other possible behaviors, which are not used in this work. As a result, it can happen that some genes perform no action.

An SU that produces a TF (SU$^{\mathrm{TF}}$) also encodes all parameters related to the TF, such as the affinity value, the decay rate D_i^c, the diffusion rate D_i^f, as well as the amount A_i of the TF$_i$ to be produced:

$$A_i(\alpha_k) = \begin{cases} \beta\left(\frac{2}{1+e^{-20 \cdot f \cdot \alpha_k}} - 1\right) & \text{if } \alpha_k > 0 \\ 0 & \text{otherwise} \end{cases}, \tag{5}$$

where f and β are both encoded in the SU$^{\mathrm{TF}}$. Which TF$_i$ is produced is defined in terms of the affinity value.

A TF produced by an SU can be partly internal and partly external. To determine how much of a produced TF is external, a percentage $(p^{\mathrm{ext}} \in (0, 1))$ is also encoded in the corresponding gene. Thus, $\Delta c_i^{\mathrm{ext}} = p^{\mathrm{ext}} \cdot A_i$ is the amount of external TF to be produced and $\Delta c_i^{\mathrm{int}} = (1 - p^{\mathrm{ext}}) \cdot A_i$ is that of the internal TF.
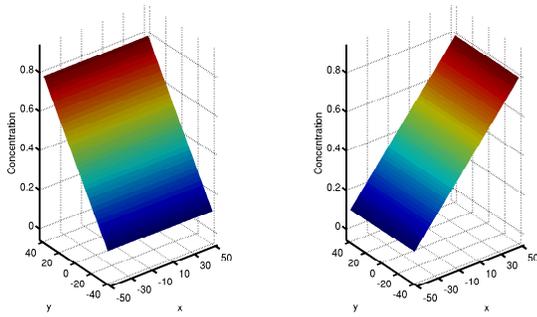
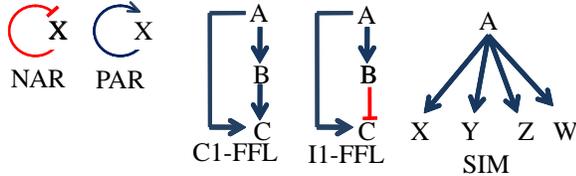Figure 2: Concentrations of the prediffused TFs.

Figure 3: Network motifs (adapted from Alon (2006)).

External TFs are put on four grid points around the center of the cell. They undergo first a diffusion and then a decay process:

$$\text{Diffusion:} \quad \mathbf{u}_i^*(t) = \mathbf{u}_i(t-1) + 0.1 D_i^f \cdot (\mathbf{G} \cdot \mathbf{u}_i(t-1)), \quad (6)$$
$$\text{Decay:} \quad \mathbf{u}_i(t) = ((1 - 0.1 D_i^c) \mathbf{u}_i^*(t)), \quad (7)$$

where $\mathbf{u}_i$ is a vector of the concentrations of the i-th TF at all grid points and the matrix $\mathbf{G}$ defines which grid points are adjoining. The internal TFs underlie only a decay process:

$$c_i^{\text{int}}(t) = (1 - 0.1 \cdot D_i^c) \, c_i^{\text{int}}(t-1). \quad (8)$$

All internal and external concentrations of TFs are limited to an interval of $[0, 1]$.

In our experiments, we put two prediffused, external TFs without decay and diffusion in the computation area. The first TF (preTF00) has a constant gradient in the y-direction and the second (preTF01) in x-direction (see Figure 2 and Figure 13).

Static and Dynamic Network Motifs

Network motifs are sub-networks that occur more often in biological gene regulatory networks than expected at random. In this work, we analyze the occurrence of different types of regulatory motifs, such as autoregulation, feed-forward-loops and single input modules, see Figure 3. In the following, we describe the function of a few network motifs, as described in Alon (2006, 2007):

- **Negative autoregulation (NAR)** defines a gene whose product directly inhibits its own expression. Such motifs can speed up the response time compared to a gene without NAR with the same steady state. It leads to steady

states with a rapid rise and a sudden saturation. NAR also promotes robustness.

- The **positive autoregulation (PAR)** slows down the response time and can lead to bi-stability.

- The **coherent feed-forward loop 1 (C1-FFL)** results in a fast convergence to a steady state but a slow decrease of the concentration.

- The **incoherent feed forward loop 1 (I1-FFL)** can act as a pulse generator. It can turn a concentration very fast on with an overshoot, and then it converges to its steady state.

- The **Single input module (SIM)** consists of one gene regulating many other genes. Temporally sequential cellular events can be controlled with a SIM.

There are a lot of different FFLs, among which C1-FFL and I1-FFL are the most frequent ones in E. coli and yeast. The functional analysis described above is performed on isolated motifs, and therefore their behavior in a whole network can be very different.

All possible connections of a GRN define the *static network*. Therefore, the *static network motifs* are all possible network motifs regardless of whether they are actually used during cell operations. In this paper, we want to analyze only the network connections that are really used during development, which constitute the *dynamic network*. The related motifs are then termed the *dynamic network motifs*. In order for a static motif to be counted as a dynamic motif, all motif connections have to have been activated (above the threshold) in at least one cell at anytime during development. Thus the dynamic motif must play an active role during cell operations and not just a potential role as the static motif. Of course dynamic motifs are a subset of static motifs.

Experimental Settings

We use an extended evolution strategy, (μ, λ)-ES with elitism for evolving the developmental model, where μ and λ are parent and offspring population size, respectively (Beyer and Schwefel, 2002). In this work, $\mu = 30$, $\lambda = 200$, and 3 elitists are adopted. The strategy parameter σ is fixed to $\sigma = 10^{-4}$ in our work.

in addition to mutation, we use gene duplication, gene transposition and gene deletion as genetic variations. Gene duplication randomly copies a sequence of RUs and SUs in the chromosome and then inserts it, again randomly, into the chromosome. In the case of gene transposition or deletion, this randomly picked out sequence of RUs and SUs is moved to another randomly chosen site on the chromosome, or simply removed.

Mutation is always performed, while gene duplication, transposition and deletion are exclusive, i.e., only one of
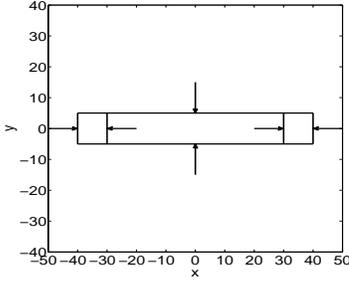
Figure 4: The target shape for the cellular growth model.

them can be performed to the same chromosome in one generation. The probabilities for gene duplication, gene transposition, and gene deletion are $p_{dup} = 0.05$, $p_{trans} = 0.02$, and $p_{del} = 0.03$. These values are not particularly motivated, however, the algorithm is not sensitive to the choice of probabilities.

The goal of the evolution is to obtain an elongated shape resulting from the cell growth process controlled by the GRN. To this end, we define a target shape, as described in Figure 4. The target shape has an approximated width-to-height ratio of $a : b$, which in the experiment, we set $a_{max} = 10$, $b_{min} = 60$ and $b_{max} = 80$. Thus, the fitness function can be defined as follows:

$$f = p_1 - p_2 - \min\left\{\min_i\left\{\boldsymbol{x}^i(1)\right\}, -\frac{a_{max}}{2}\right\}$$
$$+ \max\left\{\max_i\left\{\boldsymbol{x}^i(1)\right\}, \frac{a_{max}}{2}\right\}, \qquad (9)$$

where $\boldsymbol{x}^i$ represents the position of the i-th cell and

$$p_1 = \begin{cases} 70 + \min_i\left\{\boldsymbol{x}^i(0)\right\} & \text{if } \min_i\left\{\boldsymbol{x}^i(0)\right\} < -\frac{b_{max}}{2} \\ -30 & \text{if} -\frac{b_{max}}{2} < \min_i\left\{\boldsymbol{x}^i(0)\right\} < -\frac{b_{min}}{2} \\ \min_i\left\{\boldsymbol{x}^i(0)\right\} & \text{otherwise} \end{cases}$$
$$(10)$$

and

$$p_2 = \begin{cases} 70 + \max_i\left\{\boldsymbol{x}^i(0)\right\} & \text{if } \max_i\left\{\boldsymbol{x}^i(0)\right\} > \frac{b_{max}}{2} \\ 30 & \text{if } \frac{b_{max}}{2} > \max_i\left\{\boldsymbol{x}^i(0)\right\} > \frac{b_{min}}{2} \\ \max_i\left\{\boldsymbol{x}^i(0)\right\} & \text{otherwise} \end{cases}.$$
$$(11)$$

To achieve a computationally tractable size of the body morphology, the number of cells (n_c) is constrained between 10 and 500. A penalty of $600 - n_c$ is applied if $n_c < 10$ and a penalty of n_c if $n_c > 500$. If the cells in the developed morphology are not fully connected, this means there exists one or several cells with a high distance to all other cells, a fitness of 50 is assigned.

Experimental Results

The best and mean fitness curves of an evolutionary run are presented in Figure 5. We can observe two fitness jumps
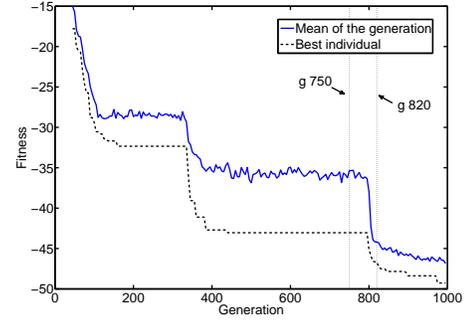

Figure 5: Fitness curves of the analyzed evolutionary run. Solid line: mean of the generation. Dotted line: best individual.
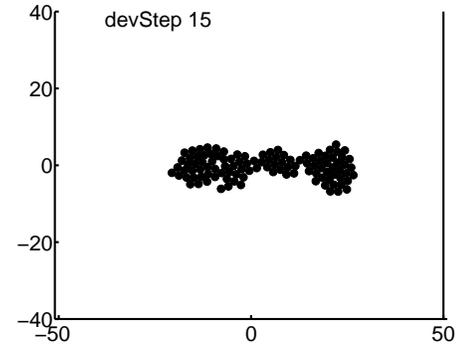

Figure 6: Resulting shape of the best individual.

around generations 350 and 800 during the whole evolution. The resulting shape of the best individual in the last generation is shown in Figure 6. The morphologies of the individuals of the first generations all result in either no cell or too many cells (we aborted the runs with more than 700 cells). In Figure 7 the total number of genes is shown. The number of genes is nearly constant, there is only one huge jump at the end of the evolution.

Dynamic Network Motifs

We count the different network motifs for all selected individuals every 5th generation. The motifs of the best individual and the mean of the parent generation are presented in Figures 8 - 11. Our algorithm counts all occurrences of one gene activating two others as one SIM (which is then a three node motif). When there is one gene activating more than two other genes, the algorithm counts more SIMs, according to the combinatorial possibilities $\binom{N}{2}$. E.g. for 4 genes
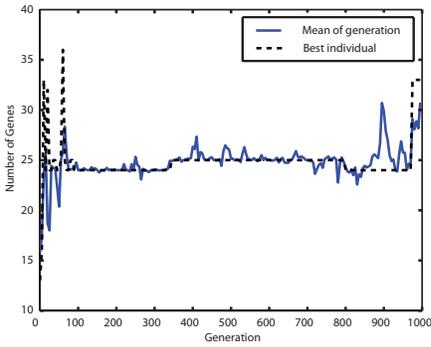
Figure 7: Number of genes of the best individual and the mean of the generation.
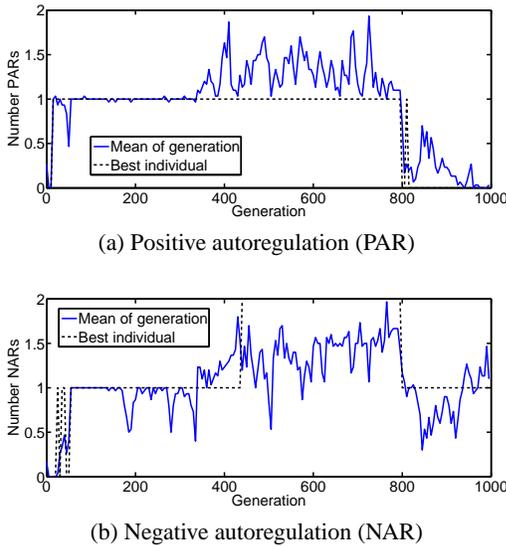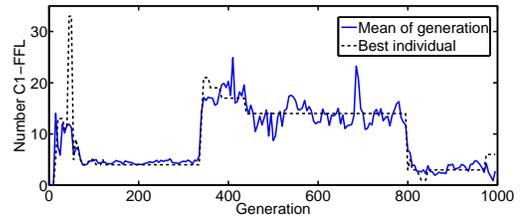

(a) Positive autoregulation (PAR)

(b) Negative autoregulation (NAR)

Figure 8: Number of autoregulations (AR).

(a) C1-FFL

(b) C1-FFL with PAR

(c) C1-FFL with NAR
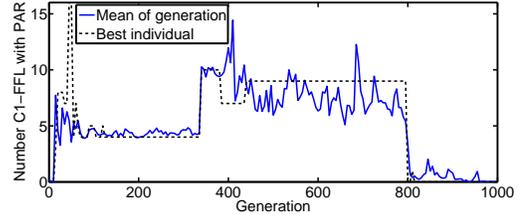
Figure 9: Number of coherent feed-forward loops (C1-FFL) with only activating connections.

our algorithm counts $\frac{4!}{2!(4-2)!} = 6$ SIMs. This masks on the one hand the number of SIMs, but on the other hand the size of the SIM is taken into account.

Regarding the number of most motifs, we find an increase in the beginning of the evolution and a decrease in later generations. An increase in the number of motifs is observed often between generation 300 and 500, while a considerable decrease of most motifs is observed around generation 800. The number of some motifs, e.g., I1-FFL, I1-FFL with NAR and SIM with NAR, increases again in the last generations, which can be explained with the increase in the number of genes (see Figure 7). The two large changes in the number of motifs correlate with two large fitness jumps. A change in the number of genes is not the reason, though the number of genes is nearly constant (see Figure 7). We hypothesize that on the one hand, evolution attempts to increase the number of motifs to perform better, whereas on the other hand, motifs that are not helpful are lost in later generations.

In the following, we discuss in greater detail the change of the number of the motifs:

- **PAR**: One PAR exists in the best individual until generation 800, then the PAR is lost. On average over the generations, the number of PAR increases between generation 300 and 400 from about one to between one and two and becomes zero around generation 800. PAR seems to be important during evolution but is lost in later generations.

- **NAR:** The number of NARs is very low throughout the evolution. It starts from one, goes up to two at about generation 450 and falls back to one again at generation 800.

- The number of **C1-FFL** is high during the evolution compared to that of the PARs and NARs. There is a considerable increase of this motif between generation 300 and 400 and a decrease around generation 800. The numbers of **C1-FFL with PAR** and **C1-FFL with NAR** are smaller but have a similar trend as **C1-FFL**.

- The number of **I1-FFL** is very low at the beginning and also increases between generation 300 and 400 to about 10 and decreases again around generation 800. At the end of the evolution, there is again an increase in the number
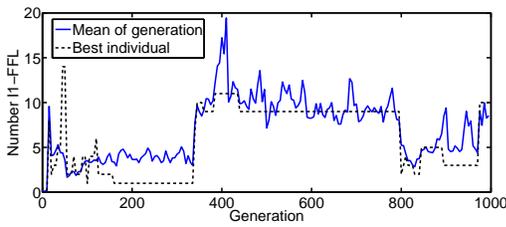
(a) I1-FFL
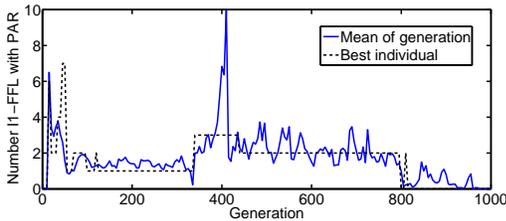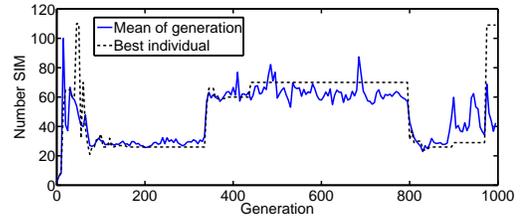

(b) I1-FFL with PAR
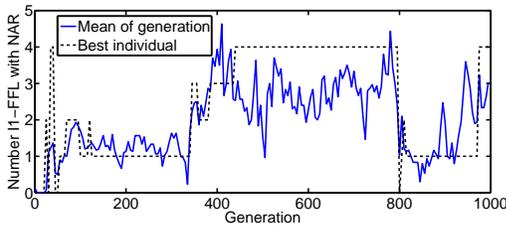
(c) I1-FFL with NAR

Figure 10: Number of incoherent feed-forward loops (I1-FFL) with one negative connection from B to C.

(a) SIM

(b) SIM with PAR

(c) SIM with NAR

Figure 11: Number of single input modules (SIM) during the evolution. We count three nodes SIMs, so that larger SIMs result in a higher number of SIMs.

of this motif. The number of **I1-FFL with PAR** and **I1-FFL with NAR** is much lower than that of the **I1-FFL**.
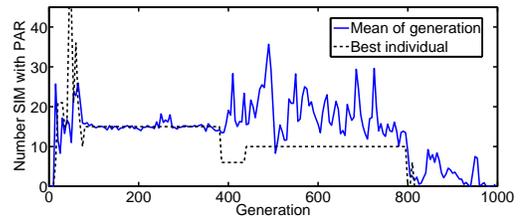
- The number of **SIMs** and **SIMs with NAR** is much higher than that of the other motifs. Note that we count all three-node SIMs, and consequently the larger the SIM, the more three node SIMs are counted. The change of SIMs during the evolution is comparable to that of the I1-FFL. The **SIM with PAR** is the only motif that decreases between generation 300 and 400, and reaches zero at generation 800 (because the PARs decrease to zero).

To relate the changes in the number of motifs to the occurrences of the genetic operators during evolution, including duplication, deletion or transposition, we traced back the ancestors of the best individual in the final generation and analyzed which genetic operators are selected over the generations. The results are given in Figure 12.
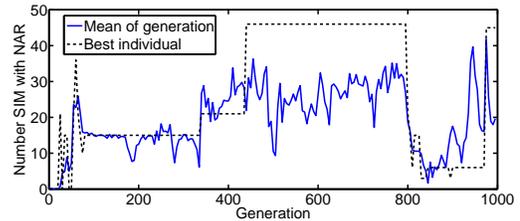
The gene deletion selected in generation 800 correlates with a strong fitness increase and a decrease of a lot of motifs. To better understand what happened during these generations, we analyze the best individual in generation 750 at the fitness plateau before the deletion and the best individual in generation 820 after the deletion in the next section.
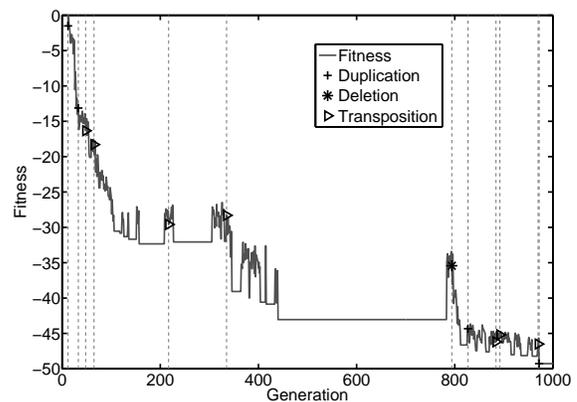

Figure 12: The fitness of the ancestors of the best individual in the last generation. Symbol '+' denotes a gene duplication, '*' a deletion and a triangle a gene transposition.
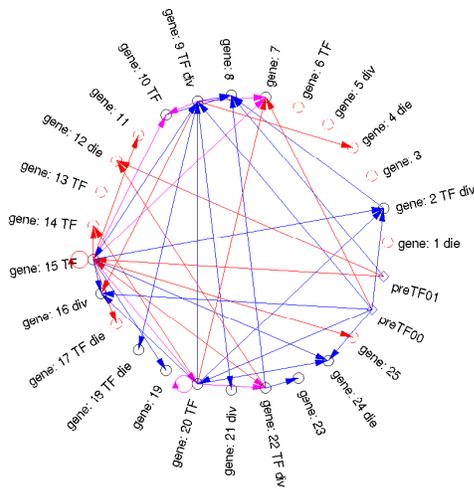
Figure 13: The genes and their used connections of the best individual in generation 750. The circles represent the different genes. Genes that are active during development are denoted with black (solid) circles. Red (dashed) circles indicate genes that are never active. The arrows represent the interactions between the genes, where blue represents an activating, red an inhibiting and magenta both an activating and inhibiting connections. The two diamonds represent the predefined TFs.

Detailed analysis of two individuals

The genes and their activations of the best individual in generation 750 and 820 are presented in Figure 13 and 14.

Note that only the dynamic activations are shown, and there are much more static activations.

The deleted regulatory and structural units belong to genes 9 and 10 of the best individual of generation 750. The SU for cell division of gene 9 and the complete gene 10 are deleted. We skipped gene number 10 in the second individual to ease the comparison of the two individuals. Another difference is that the SU of gene 20 of the best individual in generation 750 changes from TF production to an unused SU through mutation. Though gene 10 of the best individual in 750 has no further influence on the development (no arrows starting from this gene in Figure 13), the more important change seems to be the mutation of gene 20. Figure 15 shows the activations of the different genes in temporal hierarchies. The inhibitions are not shown and the inactivated genes are omitted. There are only temporal hierarchies and one feedback loop. The mutation to gene 20 resulted in a deletion of the whole sub-tree. The deletion of gene 9 has no further effect on the development. Gene 20 in the best individual of generation 750 has a lot of connections to other genes and is a member of a lot of motifs. Interestingly, the loss of gene 20 resulted in an increase in fitness from generation 750 to generation 820.
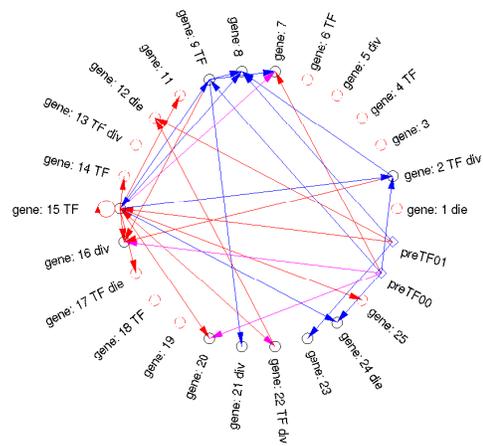

Figure 14: The genes and their used connections of the best individual 820. Notation as in Figure 13. The genes are numbered, and number 10 is skipped for an easier comparison betwen the two individuals of generation 750 and 820, because gene 10 was deleted in between.

(a) Individual 750_0
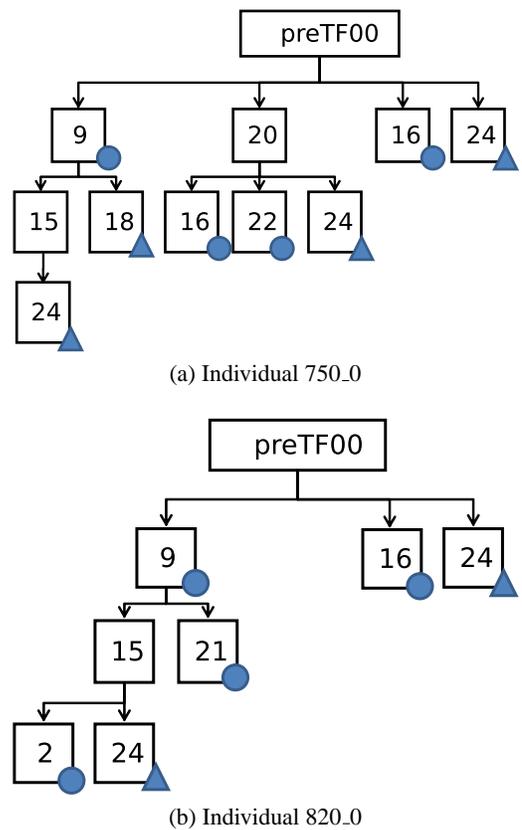

(b) Individual 820_0

Figure 15: The activating relations of the different genes. Genes for cell division are marked with a circle, genes for cell death with a triangle. Only some important activating effects are shown, inactivated genes and inhibiting connections are omitted.

Summary and Conclusion

In this work, we have analyzed the change in the number of network motifs in the gene regulatory network during evolution of a cell growth model for an elongated body morphology. A general trend is that the overall number of motifs increases significantly at the beginning of evolution. During the evolutionary process the numbers of all motifs have increased with the exception of PAR.

Since the genome length does not change significantly during evolution, it seems that it is not just the increase of genetic material but of structured genetic material, i.e., dynamic network motifs, that is important during the evolutionary process. At the same time, motifs that do not influence development are lost again during evolution. Therefore, it seems that the frequency of motifs is under selectional control and that the increase of dynamic network motifs is related to the evolvability of the process.

We analyzed the genetic changes that contributed to the fitness jump around generation 800 and compared the genes of two individuals before and after the genetic change. We found that the fitness increase and the decrease of the number of dynamic motifs were due to one mutation that changed a gene from producing an important TF to a gene without function. Contrary to intuition, the correlated gene deletion neither influenced the fitness nor the number of motifs.

A more detailed interpretation of our results is restricted by the fact that only observations from one experiment are available. Needless to say that a more statistically sound analysis would be desirable, however, the considerable computational expense of the described process makes it difficult to run a larger number of experiments.

For the analysis of static motifs, other authors have normalized their results to the motifs one can find in random networks (Kashtan and Alon, 2005). For dynamic motifs this is difficult, because most static motifs in random networks will not be dynamical, simply because the developmental process terminates very early. Frequently, this is due to the early activation of cell death by a prediffused TF in random networks. More precise, most random networks result in an activation of cell death in the first developmental step and the development stops. This results in nearly no network motifs, because no TFs are produced. In order to make sure that during the evolutionary process not just the raw genetic material is increased we compared the number of dynamic motifs to the genome length during evolution.

Acknowledgements

References

Alon, U. (2006). *An Introduction to Systems Biology: Design Principles of Biological Circuits*. Chapman & Hall.

Alon, U. (2007). Network motifs: theory and experimental approaches. *Nature Reviews Genetics*, 8:450–461.

Andersen, T., Newman, R., and Otter, T. (2009). Shape homeostasis in virtual embryos. *Artificial Life*, 15(2):161–183.

Babu, M. M., Luscombe, N. M., Aravind, L., Gerstein, M., and Teichmann, S. A. (2004). Structure and evolution of transcriptional regulatory networks. *Current Opinion in Structural Biology*, 14(3):283–291.

Beyer, H.-G. and Schwefel, H.-P. (2002). Evolution strategies –a comprehensive introduction. *Natural Computing: an international journal*, 1(1):3–52.

de Jong, H. (2002). Modeling and simulation of genetic regulatory systems: A literature review. *Journal of Computational Biology*, 9(1):67–103.

Eggenberger Hotz, P., Gómez, G., and Pfeifer, R. (2003). Evolving the morphology of a neural network for controlling a foveating retina - and its test on a real robot. In *The Eighth International Conference on Artificial Life*, pages 243–251. MIT Press.

Geard, N. and Willadsen, K. (2009). Dynamical approaches to modeling developmental gene regulatory networks. *Birth Defects Research Part C*, 87(2):131–142.

Harding, S. and Banzhaf, W. (2008). Artificial development. In Würz, R. W., editor, *Organic Computing*, chapter 9, pages 201–219. Springer.

Jin, Y., Schramm, L., and Sendhoff, B. (2008). A gene regulatory model for the development of primitive nervous systems. In *Proc. of ICONIP 2008*, pages 48–55. Springer.

Joachimczak, M. and Wròbel, B. (2009). Evolution of the morphology and patterning of artificial embryos: scaling the tricolour problem to the third dimension. In *Proc. of ECAL 09*.

Kashtan, N. and Alon, U. (2005). Spontaneous evolution of modularity and network motifs. *Proceedings of the National Academy of Sciences*, 102(39):13773–13778.

Kwon, Y. K. and Cho, K. H. (2008). Quantitative analysis of robustness and fragility in biological networks based on feedback dynamics. *Bioinformatics*, 7(24):987–994.

Schramm, L., Jin, Y., and Sendhoff, B. (2009). Emerged coupling of motor control and morphological development in evolution of multi-cellular animats. In *Proc. of ECAL 09*.

Steiner, T., Schramm, L., Jin, Y., and Sendhoff, B. (2007). Emergence of feedback in artificial gene regulatory networks. In *Proc. of CEC*, pages 867–874.

Steiner, T., Trommler, J., Brenn, M., Jin, Y., and Sendhoff, B. (2009). Global shape with morphogen gradients and motile polarized cells. In *Proceedings of the 2009 Congress on Evolutionary Computation*, pages 2225–2232.

Wolpert, L. (2004). *Principles of Development*. Oxford University Press.